J. Micropalaeontology, 43, 423–439, 2024
https://doi.org/10.5194/jm-43-423-2024

Journal of Micropalaeontology
Open Access

Early Triassic conodonts from the Liangshan area, Hanzhong, Shaanxi, South China

Yueli Zhao[1], **Yanlong Chen**[1], **Jianqiang Wang**[1], **Xinyi Ma**[2], **Chunling Xue**[1], **Timothy P. Topper**[1,3], and **Zhifei Zhang**[1]

[1]State Key Laboratory of Continental Dynamics, Shaanxi Key Laboratory of Early Life and Environments and Department of Geology, Northwest University, Xi'an, 710069, China
[2]School of Earth Sciences and Engineering, Nanjing University, Nanjing, 210023, China
[3]Department of Palaeobiology, Swedish Museum of Natural History, Stockholm, 10405, Sweden

Correspondence: Yanlong Chen (yanlong.chen@nwu.edu.cn)

Received: 7 February 2024 – Revised: 31 July 2024 – Accepted: 5 August 2024 – Published: 10 October 2024

Abstract. The Liangshan area in Hanzhong city, Shaanxi Province, China, is in the northwestern part of the Yangtze Platform. Strata across the Permian–Triassic boundary (PTB) are continuous, well developed, and fossiliferous, providing an ideal place for biostratigraphic study. However, there is a dearth of reliable conodont biostratigraphic data from PTB sequences in the Liangshan area. In this study, conodonts are examined at the Zhangkouzi and Chencun sections in the Liangshan area. Three conodont species are documented from the Zhangkouzi section, *Hindeodus parvus*, *H. sosioensis*, and *H. postparvus*, and six conodont species are documented from the Chencun section, *Pachycladina multidentata*, *Pa. costatus*, *Pa. magnus*, *Pa. bidentata*, *Foliella formosa*, and *Neospathodus concavus*. Based on the stratigraphic distribution of conodonts, the Zhangkouzi section is Changhsingian–Griesbachian (early Induan) in age, and the Chencun section is Smithian (early Olenekian) in age. Our data suggest that the genus *Foliella* evolved from the genus *Pachycladina*, that *F. gardenae* evolved from *F. formosa*, and that the latter evolved from *Pa. multidentata*. The multi-element apparatus of *Pachycladina* is reconstructed with 15 elements.

1 Introduction

The end-Permian mass extinction (251.939 ± 0.031 Ma; Burgess et al., 2014; Shen et al., 2019) was the largest biological crises on Earth and had a significant impact on both marine and terrestrial ecosystems (Raup, 1979; Jablonski, 1994; Retallack, 1995; Shen et al., 2011; Song et al., 2014, 2018; Stanley, 2016; Fan et al., 2020; Xu et al., 2021). The Permian–Triassic boundary (PTB) has received widespread attention, as we attempt to understand the causes and consequences of the end-Permian mass extinction.

Conodonts, bivalves, and ammonoids are significant taxa for both stratigraphic correlation and the definition of the PTB (Song et al., 2013; Song and Tong, 2016; Dal Corso et al., 2022). The Global Stratotype Section and Point (GSSP) of the PTB was defined in 2001, by the first appearance datum (FAD) of *Hindeodus parvus* at Meishan D section, Changxing County, Zhejiang Province, South China (Yin et al., 2001; Zhao et al., 2008). However, *H. parvus* has not been recorded in the Liangshan area in previous studies (Lu, 1956; Wu, 1957; Kanmera and Nakazawa, 1973; Wang, 1978; Liu, 1982; Rui, 1984; Guo et al., 2016); thus, the precise location of the PTB in this area is unknown.

The Liangshan area in southern Shaanxi, part of the Upper Yangtze Platform (Fig. 1b), is one of the most important areas for the study of Permian–Triassic strata. The Permian–Lower Triassic strata in the Liangshan area are continuous, well developed, and fossiliferous. Studies on the Permian and Triassic strata in the Liangshan area can be dated back to the 1950s (e.g. Lu, 1956; Wu, 1957). Previous research in this area was mainly focused on stratigraphic correlation (Lu, 1956; Kanmera and Nakazawa, 1973; Liu, 1982) and describing the rich fossil assemblages (including conodonts, corals, bivalves and brachiopods) (Wu, 1957; Chen, 1978; Wang, 1978; Chen and Li, 1979; Guo et al., 2016). Conodonts of the Early Triassic, however, are poorly studied, and

Published by Copernicus Publications on behalf of The Micropalaeontological Society.

the index fossil *Hindeodus parvus* that marks the PTB has never been reported.

Here we report conodont taxa from the Chencun and Zhangkouzi sections in the Liangshan area, Hanzhong city, Shaanxi Province. In addition to conodonts (Figs. 3–9), gastropods and ostracods have been documented (Fig. 10) in an attempt to provide a reliable biostratigraphic framework for the Permian–Triassic strata in this area.

2 Geological setting

The Liangshan area is located in the northwestern Yangtze block (Fig. 1a, b), bounded to the north by the Mianlüe suture zone (Zhang et al., 2001, 2004; He et al., 2016), and connected to the Qinling orogenic belt (Guo et al., 2016). During the Permian–Triassic transition, the Yangtze block was located near the eastern part of the Palaeo-Tethys Ocean (Fig. 1a), and the PTB strata are relatively complete in the Middle and Upper Yangtze Platform (Feng et al., 2017). The Lopingian strata comprise the Changhsing or Dalong formations, and the Lower Triassic strata consist of the Daye (equivalent to the Feixianguan Formation) and Jialingjiang formations (Zhang and Tong, 2010; Yang et al., 2012; Zhao et al., 2015; Feng et al., 2017; Miao et al., 2021; Shen et al., 2021).

Within the Liangshan area, the strata of Permian–Lower Triassic are well exposed. A major transgression occurred in the Upper Yangtze Platform during the late Lopingian (He et al., 2016), resulting in the deposition of the Wuchiaping and Changhsing formations (He and Luo, 2010). The Daye Formation of the Lower Triassic in the Liangshan area belongs to the transitional facies of Daye and Feixianguan formations. The lower part of the Daye Formation is composed of light grey, light yellow micritic, bioclastic limestone, marl, and shale, and the upper part is composed of thin purple shale and oolitic limestone, indicating deposition in neritic facies (Huo, 1960; Rui et al., 1984; Jian et al., 1992; Liu et al., 1996; Zheng et al., 2021).

The studied Zhangkouzi section (106°54′00″ N, 33°4′48″ E; Figs. 1c, 2) is located about 1 km to the southeast of Chenjiacun Lake, is exposed along a bituminous road with a total thickness of 83 m, and consists of continuous strata from the Changhsing to Daye formations. The Changhsing Formation is mostly limestones and shales, and the Daye Formation is thin-bedded limestone and shale and yields conodonts, gastropods, and ostracods. The Chencun section (106°53′24″ N; 33°5′24″ E; Figs. 1c, 2) is also located along a bituminous road on the southern bank of the Chenjiacun Lake with a total thickness of 18.5 m and is exclusively composed of the Daye Formation, which primarily consists of thin-bedded shale and oolitic limestone with abundant conodonts. Permian–Lower Triassic strata in the Liangshan area are continuous and fossiliferous, providing an ideal opportunity to study conodont evolution and biostratigraphy across the PTB.

3 Materials and methods

In total, 84 kg of samples (each sample ranges from 3 to 6 kg) was collected for this study. In the Zhangkouzi section, 17 samples were collected from the Changhsing Formation, while one sample was collected from the Daye Formation. In the Chencun section, three samples were collected from the Daye Formation. All samples were crushed into ca. 5 cm^3 fragments and dissolved in plastic buckets with dilute acetic acid (ca. 8 %–10 %; Jeppsson et al., 1985; Jeppsson and Anehus, 1999). The insoluble residues at the bottom of buckets were sieved using 1 mm and 64 µm meshes; undissolved samples were put back into the plastic buckets to continue the dissolution process. Residues in the sieve of 64 µm meshes were collected in a beaker and dried naturally. Conodonts were concentrated in sodium polytungstate and handpicked from dried residues using a wet brush pen under a binocular microscope. A Phenom XL G2 scanning electron microscope was used for photographing the gold-coated conodont, gastropod, and ostracod specimens (Figs. 3–10) at the Department of Geology, Northwest University, Xi’an, China. All of these studied specimens are deposited at the Department of Geology (catalogue nos. 1001–1072).

4 Discussion

4.1 The Permian–Triassic boundary in the Zhangkouzi section

The PTB is typically defined by the FAD of *Hindeodus parvus*, and in the Zhangkouzi section the lowest occurrence of *H. parvus* (Fig. 2) is in rock sample ZKZ-8. However, in the Zhangkouzi section the first occurrence of *H. parvus* co-occurs with *H. sosioensis* and *H. postparvus*, two species that typically first occur in slightly younger strata (Kozur, 2003; Tong et al., 2003; Zhao et al., 2007; Jiang et al., 2014). The combination of *H. parvus*, *H. sosioensis*, and *H. postparvus* suggests that sample ZKZ-8 correlates with the *H. sosioensis* zone (Jiang et al., 2014) that occurs in the basal part of Triassic, which is slightly younger than the PTB. As such, despite sample ZKZ-8 yielding the first occurrence of *H. parvus*, the PTB in the Zhangkouzi section should be placed below the sampled horizon ZKZ-8.

4.2 The age of the Chencun section

Conodonts obtained from the Chencun section include *Pa. costatus*, *Pa. multidentata*, *Pa. magnus*, *Pa. bidentata*, *F. formosa*, and *Ns. concavus*. *Neospathodus concavus* was previously reported by Zhao et al. (2007) in the West Pingdingshan section, Chaohu, Anhui Province. In this section (Zhao et al., 2007), *Ns. concavus* occurs in the *Ns. waageni waageni*

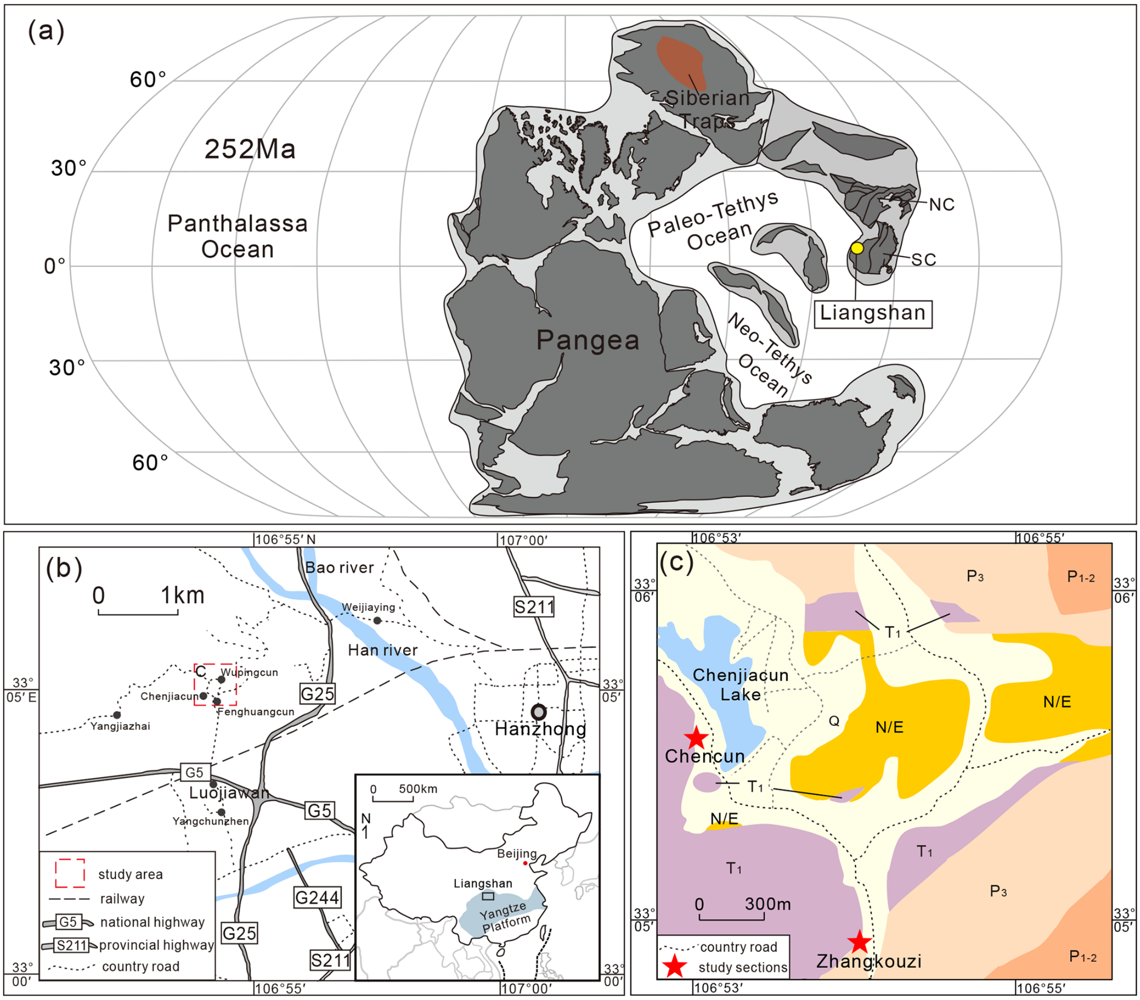

Figure 1. Location of the studied sections in the Liangshan area, Hanzhong, Shaanxi Province. **(a)** Palaeogeographic reconstruction during the end Permian to Early Triassic (modified after Huang et al., 2018; Dal Corso et al., 2022). SC stands for South China, and NC stands for North China. **(b)** Map of the Liangshan area. **(c)** Geological map of the study area. Q stands for Quaternary, N/E represents Neogene and Paleogene, T_1 is the Lower Triassic, P_3 is the Lopingian, and P_{1-2} is the Cisuralian and Guadalupian.

subzone (of the *Ns. waageni* Zone), which is early Olenekian in age (Maekawa et al., 2016; Lyu et al., 2023). An early Olenekian age is further supported by the presence of the genera *Foliella* and *Pachycladina* that have both been documented as occurring in the Smithian (Kolar-Jurkovšek, 1996; Song, 2012; Wu et al., 2021). Based on our conodont data, the Daye Formation at the Chencun section is Smithian (early Olenekian) in age.

4.3 The evolution of *Pachycladina* and *Foliella*

Two genera, *Foliella* and *Pachycladina*, of the family Ellisoniidae were recognized in the Chencun section (Figs. 3–7). The origin of *Foliella* has been debated (Orchard, 2007). Orchard (2007) suggested that *Foliella* may have evolved from the genus *Furnishius*, but our data provide another possibility. The P_1 element of *Foliella* is a platform with only two processes; however, the P_1 element of *Furnishius* normally consists of three processes and has a "Y"-shaped keel. Meanwhile, *Foliella* differs from *Furnishius* in bearing regularly arranged and uniformly sized nodes on the oral surface. The morphological differences between *Foliella* and *Furnishius* are considerable, so it is unlikely that they have a direct evolutionary relationship.

Foliella and *Pachycladina*, on the other hand, share numerous morphological similarities. On the oral surface, the carina of both *Pachycladina* and *Foliella* are well developed, with a centrally located cusp. On the aboral surface, both *Pachycladina* and *Foliella* have a keel without an obvious furrow or basal pit. Stratigraphically, *Pachycladina* is slightly older, occurring in the *Pachycladina–Hadrodontina* zone, which is Griesbachian to early Smithian in age (Perri, 1991; Kolar-Jurkovšek and Jurkovšek, 2019; Wu et al., 2019, 2021), while *Foliella* is Smithian in age (Perri, 1991; Kolar-

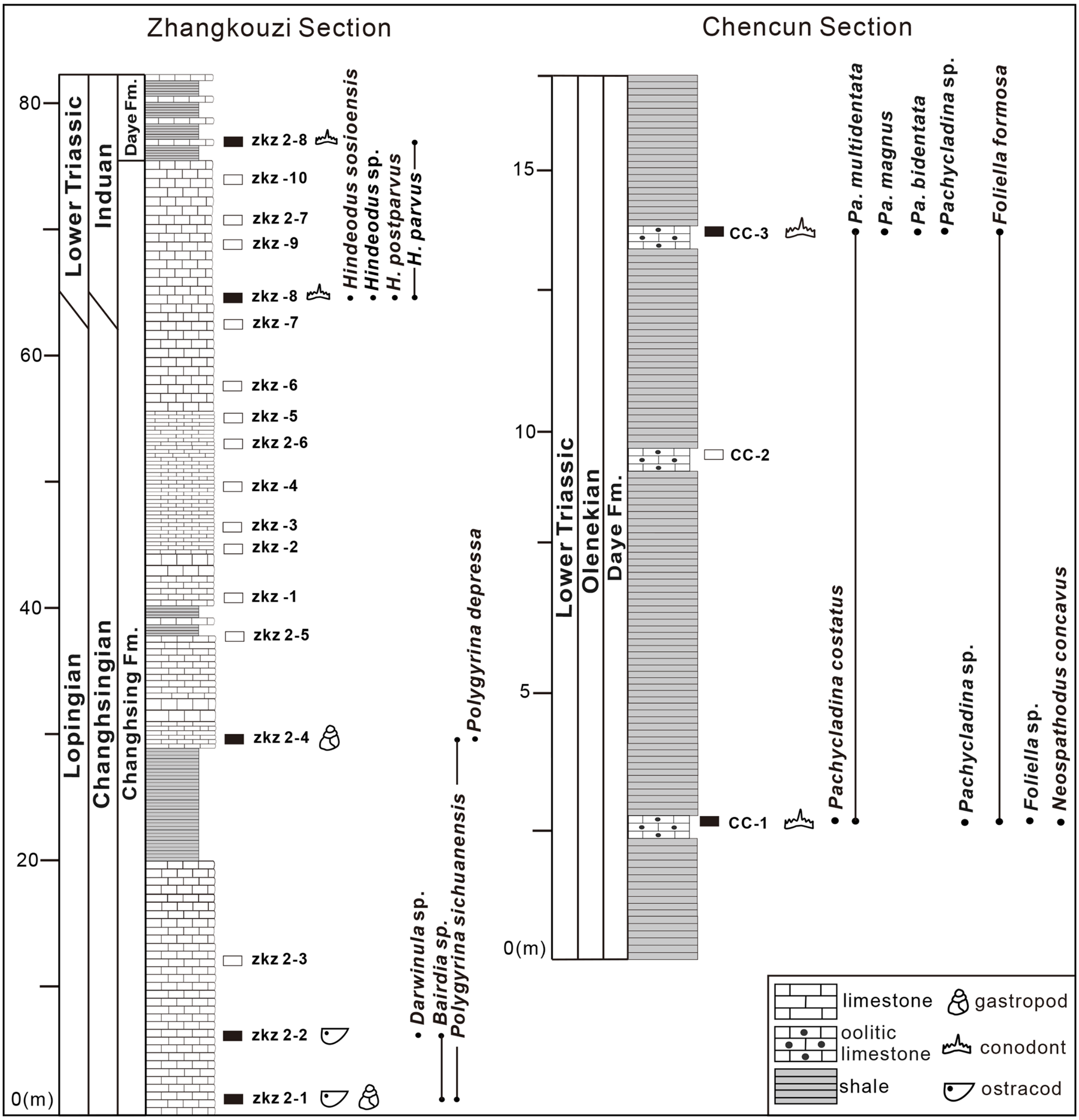

Figure 2. Lithology and stratigraphic ranges of taxa through the Zhangkouzi and Chencun sections. Black rectangles indicate productive samples. Blank rectangles indicate barren samples. *H.* stands for *Hindeodus* and *Pa.* stands for *Pachycladina*.

Jurkovšek and Jurkovšek, 2019; Wu et al., 2019, 2021). Based on their close morphological similarity and stratigraphic relationship, we propose that *Foliella* evolved from *Pachycladina*, with an evolutionary lineage from *Pachycladina multidentata* to *Foliella formosa* and to *Foliella gardenae* (Fig. 11).

4.4 The multi-element apparatus of *Pachycladina*

In previous studies, the ellisonid genus *Pachycladina* was described by seximembrate apparatus (Perri and Andraghetti, 1987; Zhang and Yang, 1991; Kolar-Jurkovšek, 1996; Song, 2012; Wu et al., 2021); however, no natural assemblage or clusters have been documented to support the seximembrate apparatus theory. Sun et al. (2020) reported three well-preserved natural assemblages and confirmed that ellisonid genus *Hadrodontina* had a multi-element apparatus composed of 15 elements. Koike (2016) described five ellisonid genera (*Furnishius, Staeschegnathus, Cornudina, Ellisonia*, and *Hadrodontina*) with septimembrate apparatus containing 15 elements. Because both *Hadrodontina aequabilis* and

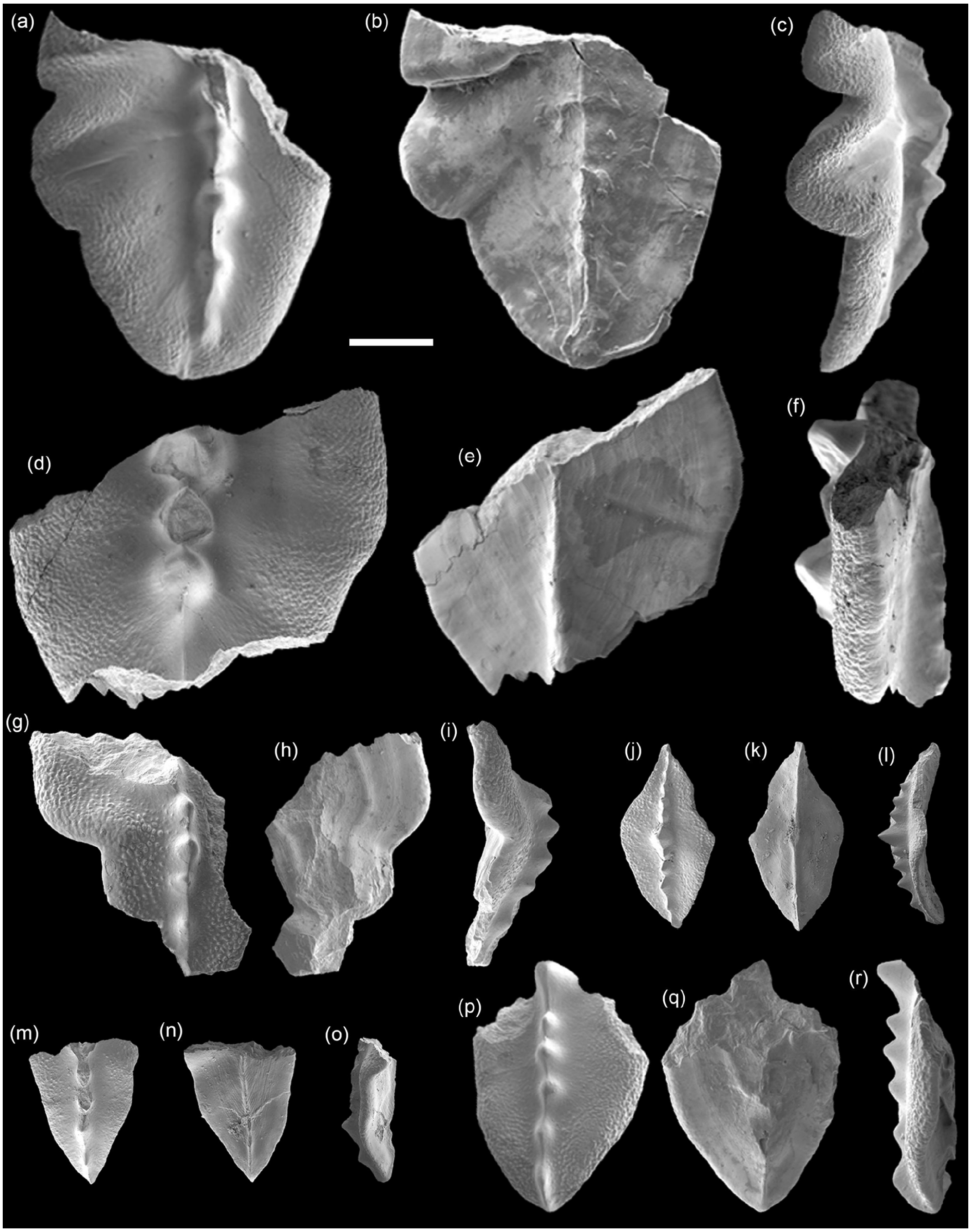

Figure 3. SEM photos of *Foliella formosa* (Tian, 1983) P_1 elements from the Daye Formation, Chencun section. **(a–c)** 1001, **(d–f)** 1002, **(g–i)** 1003, **(j–l)** 1004, **(m–o)** 1005, and **(p–r)** 1006. Panels **(a)**–**(i)** and **(p)**–**(r)** are from sample CC-1, and panels **(j)**–**(o)** are from sample CC-3. The scale bar represents 500 µm.

Pachycladina belong to the same subfamily Hadrodontinae (Koike, 2016), we recognize *Pachycladina* as possessing 15 elements (paired P_1, P_2, M, S_1, S_2, S_3, and S_4 elements and unpaired S_0 elements).

Almost all P_1 elements (accounts for 99 % of the total assemblage) from rock samples CC-1 and CC-3 belong to the *Pachycladina–Foliella* lineage, and thus almost all the P_2, S, and M elements can be assigned to the *Pachycladina–Foliella* lineage. Because *Foliella* is a descendent of *Pachycladina*, their P_2, S, and M elements should be similar. The presence of multiple species from the same sample complicates the assignment of S and M elements to specific species, especially in the absence of natural assemblages. Consequently, we have used open nomenclature (*Pachycladina* sp.) to deal with

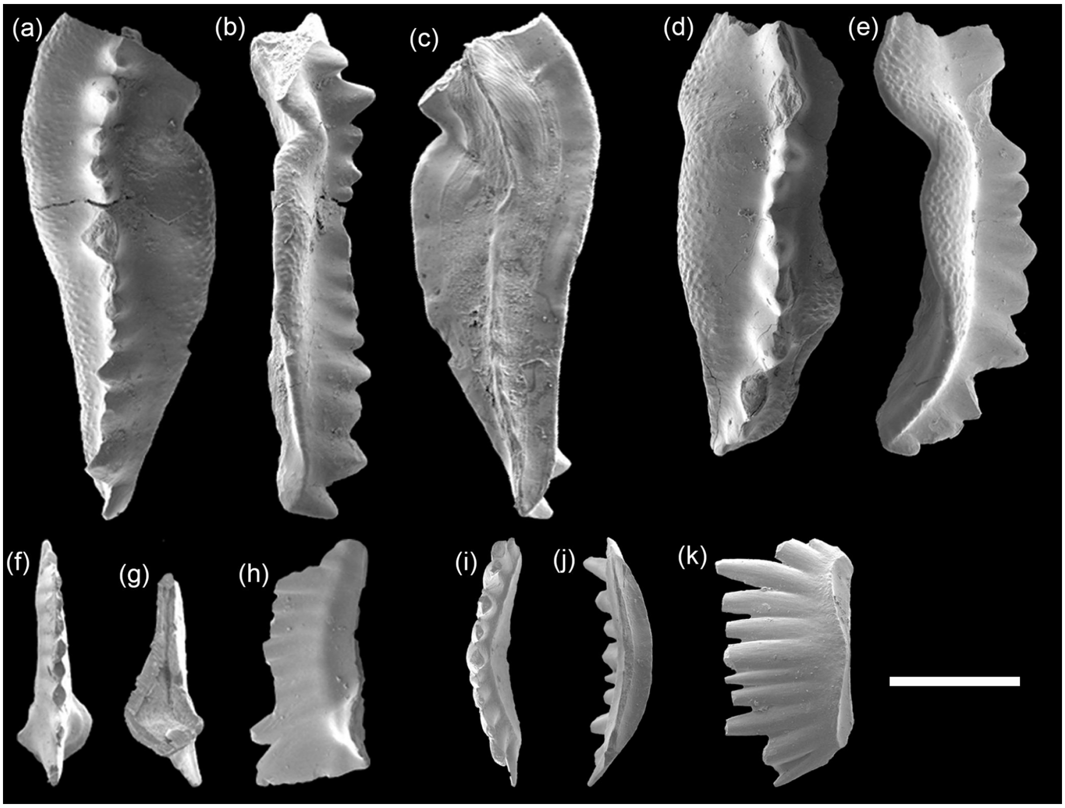

Figure 4. SEM photos of conodonts from the Daye Formation, Chencun section. **(a–e)** *Foliella* sp. P_1 elements: **(a–c)** 1007 and **(d–e)** 1008. **(f–k)** *Neospathodus concavus* Zhao and Orchard, 2007: **(f–h)** P_1 element 1009 and **(i–k)** S_0 element 1010. All are from sample CC-1. The scale bar represents 500 µm.

these ramiform elements from the CC-1 and CC-3 of Chencun section. Here we reconstruct the apparatus of *Pachycladina*, tentatively including all ramiform elements from these two rock samples, which may also include ramiform elements of *Foliella*.

5 Conclusions

In this study, a total of 4 genera and 11 conodont species were recognized in the Zhangkouzi and Chencun sections, Liangshan area, Hanzhong city, Shaanxi Province.

In the Zhangkouzi section, the lowest occurrence of *H. parvus* is associated with *H. sosioensis* and *H. postparvus*, correlating to the *H. sosioensis* zone, indicating a basal Triassic age. The conodont assemblage of *Pa. multidentata*, *Pa. bidentata*, *F. formosa*, and *Ns. concavus* suggests that the Chencun section is Smithian (early Olenekian) in age.

Our data support the idea that the genus *Foliella* evolved from the genus *Pachycladina* with an evolutionary lineage from *Pachycladina multidentata* to *Foliella formosa* and then to *Foliella gardenae*. The multi-element apparatus of *Pachycladina* is reconstructed with 15 elements with paired P_1, P_2, M, S_1, S_2, S_3, and S_4 elements and unpaired S_0 elements.

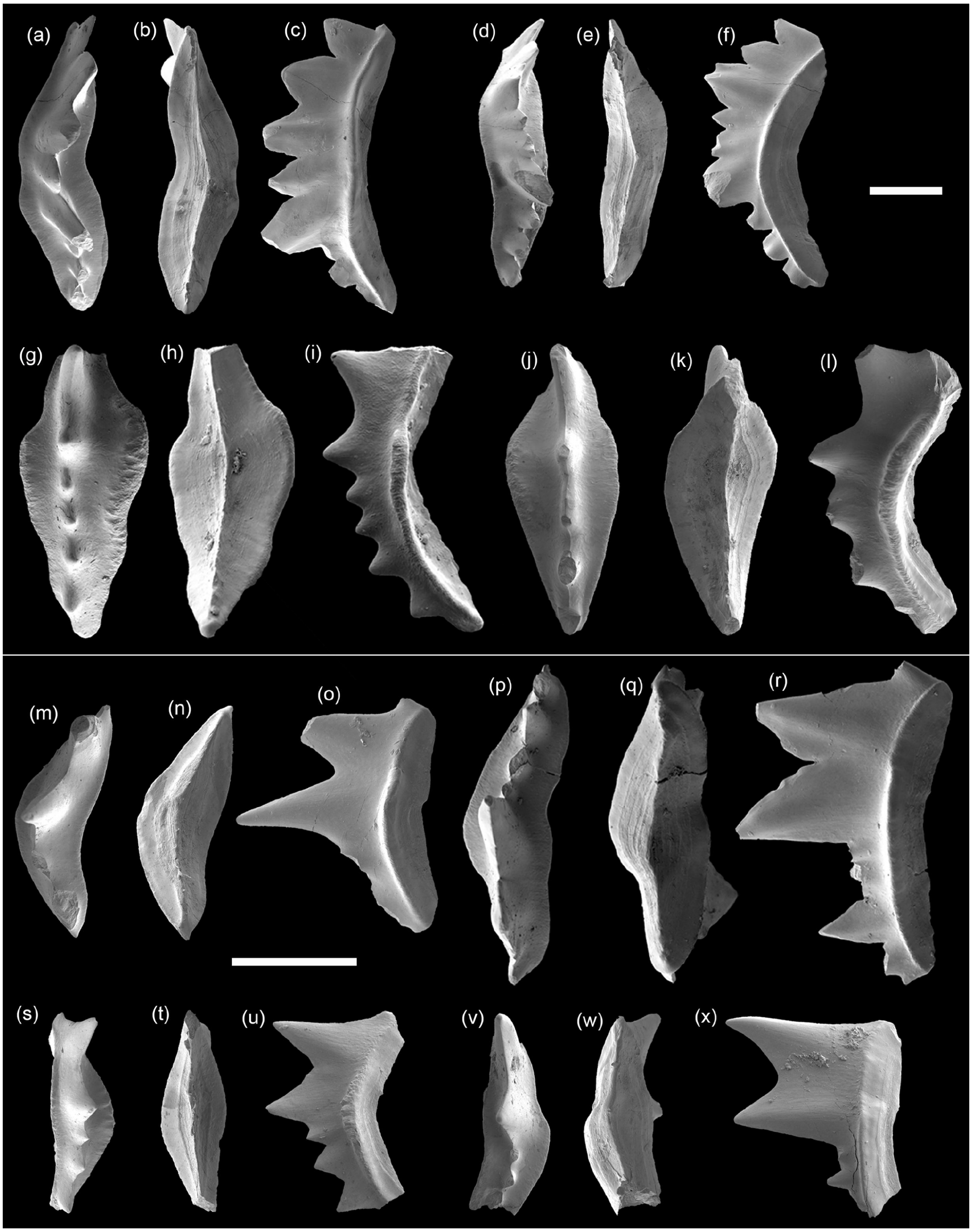

Figure 5. SEM photos of conodonts from the Daye Formation, Chencun section. **(a–f)** *Pachycladina costatus* (Tian, 1983) P_1 elements: **(a–c)** 1011 and **(d–f)** 1012. **(g–l)** *Pachycladina magnus* (Tian, 1983) P_1 elements; **(g–i)** 1013 and **(j–l)** 1014. **(m–x)** *Pachycladina bidentata* Wang and Cao, 1981 P_1 elements: **(m–o)** 1015, **(p–r)** 1016, **(s–u)** 1017, and **(v–x)** 1018. Panels **(a)**–**(f)** are from sample CC-1, and panels **(g)**–**(x)** are from sample CC-3. The scale bar represents 500 µm.

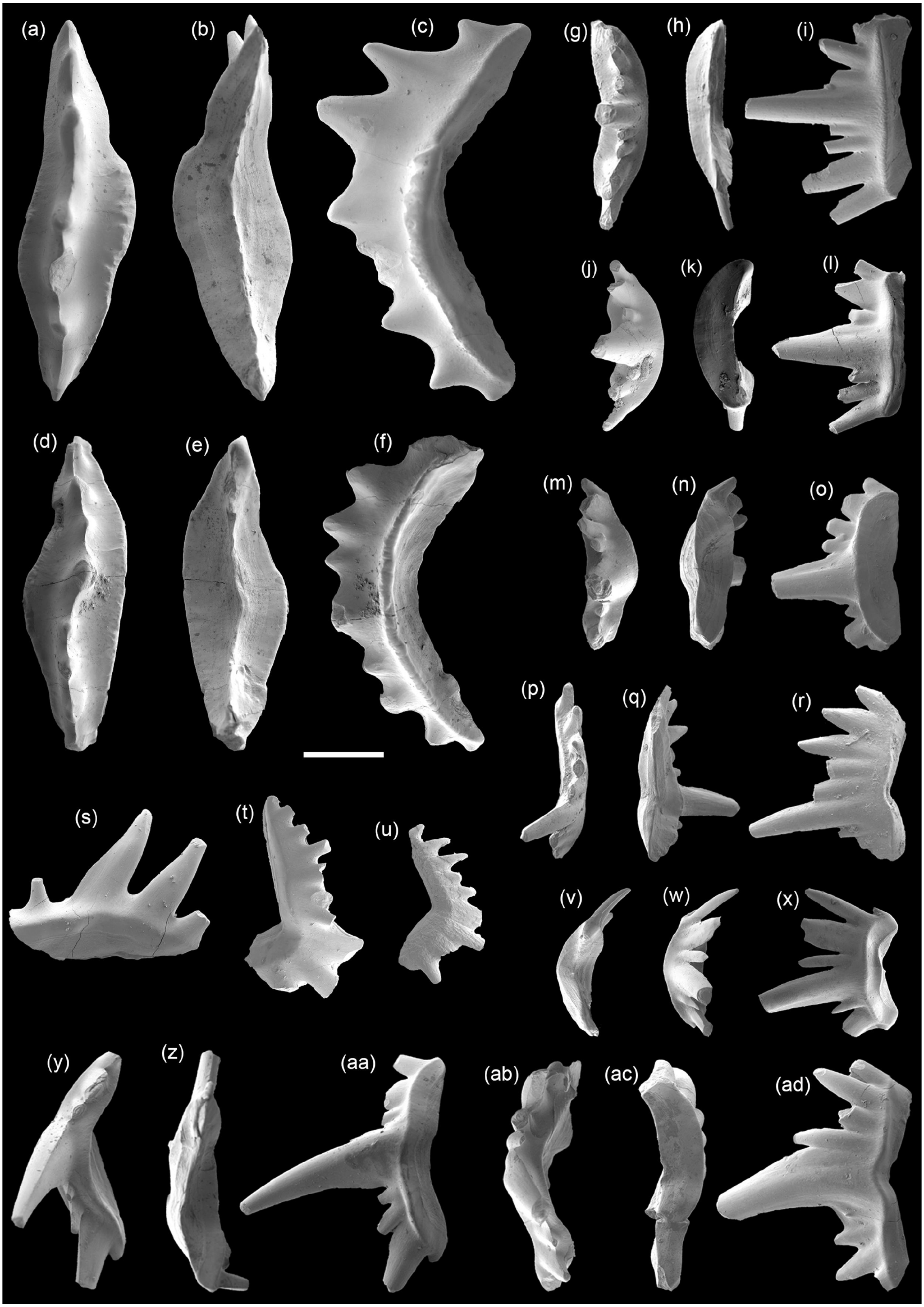

Figure 6. SEM photos of conodonts from the Daye Formation, Chencun section. **(a–f)** *Pachycladina multidentata* Wang and Cao, 1981 P_1 elements: **(a–c)** 1019 and **(d–f)** 1020. **(g–ad)** *Pachycladina* sp. **(g–l)** S_0 elements **(g–i)** 1021 and **(j–l)** 1022, as well as **(m–o)** S_1 element 1023. Panels **(p)**–**(r)** and **(v)**–**(x)** show S_2 elements **(p–r)** 1024 and **(v–x)** 1025. **(s)** P_2 element 1026; M elements **(t)** 1027 and **(u)** 1028; **(y–aa)** S_3 element 1029. **(ab–ad)** S_4 element 1030. Panels **(a)**–**(i)**, **(m)**–**(o)**, **(s)**, **(v)**–**(x)**, and **(ab)**–**(ad)** are from sample CC-3, and panels **(j)**–**(l)**, **(p)**–**(r)**, **(t)**–**(u)**, and **(y)**–**(aa)** are from sample CC-1. The scale bar represents 500 µm.

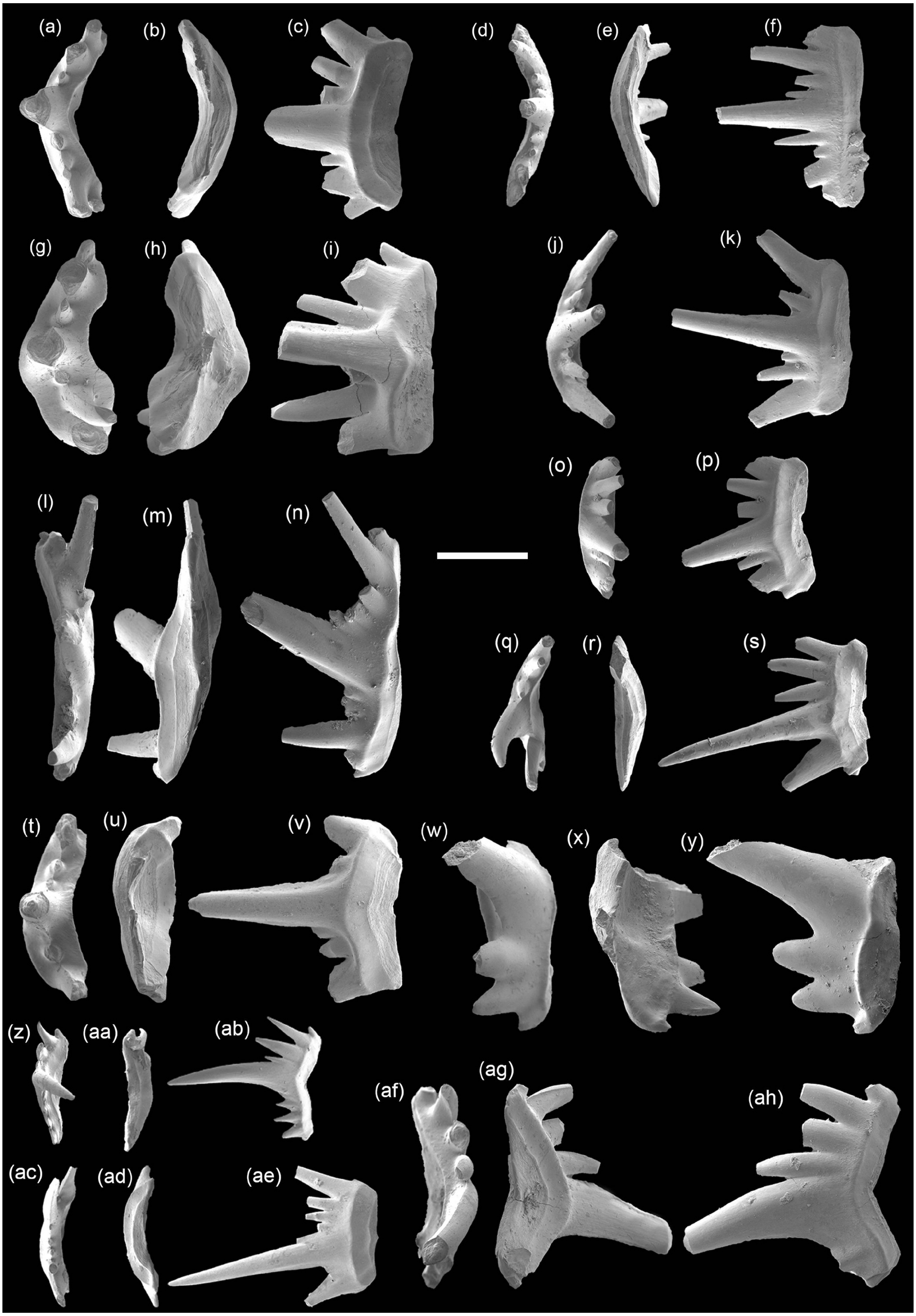

Figure 7. SEM photos of *Pachycladina* sp. from the Daye Formation, Chencun section. Panels **(a)**–**(k)** and **(t)**–**(v)** are S_0 elements: **(a–c)** 1031, **(d–f)** 1032, **(g–i)** 1033, **(j–k)** 1034, and **(t–v)** 1035; **(w–y)** S_1 element 1036 and **(l–n)** S_3 element 1037. Panels **(o)**–**(s)** and **(z)**–**(ah)** are S_2 elements: **(o–p)** 1038, **(q–s)** 1039, **(z–ab)** 1040, **(ac–ae)** 1041, and **(af–ah)** 1042. Panels **(a)**–**(c)** and **(o)**–**(v)** are from sample CC-1, and panels **(d)**–**(n)** and **(w)**–**(ah)** are from sample CC-3. The scale bar represents 500 µm.

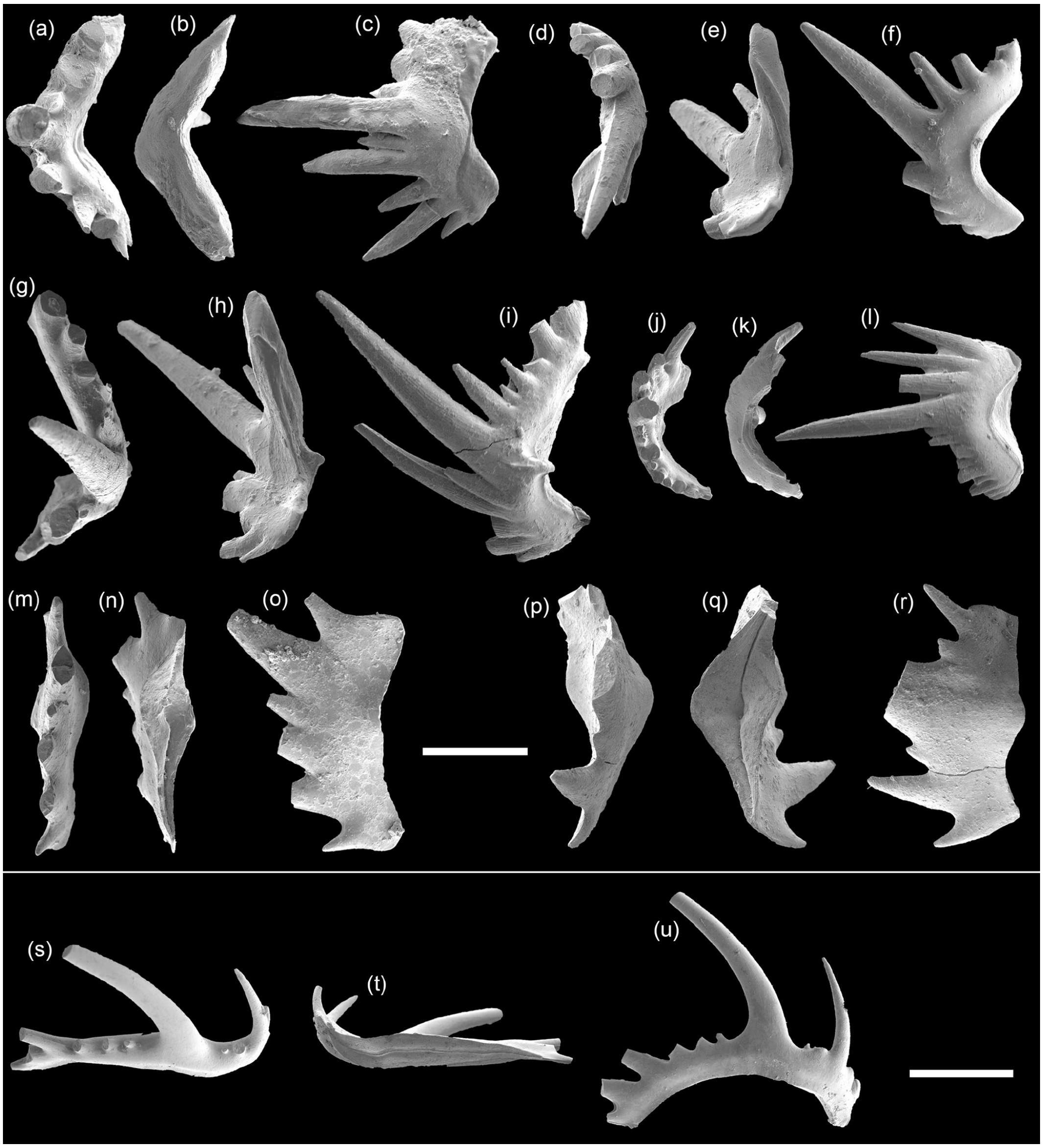

Figure 8. SEM photos of *Hindeodus* sp. from the Chanshing Formation, Zhangkouzi section. Panels **(a)**–**(c)** and **(j)**–**(l)** are S_0 elements: **(a–c)** 1043 and **(j–l)** 1044. **(d–f)** M element 1045. **(g–i)** S_{1-2} element 1046. Panels **(m)**–**(o)** and **(p)**–**(r)** are P_2 elements: **(m–o)** 1047 and **(p–r)** 1048. Panels **(s)**–**(u)** are S_{3-4} element 1049. All are from sample ZKZ-8. The scale bars represent 200 µm **(a–r)** and 500 µm **(s–u)**, respectively.

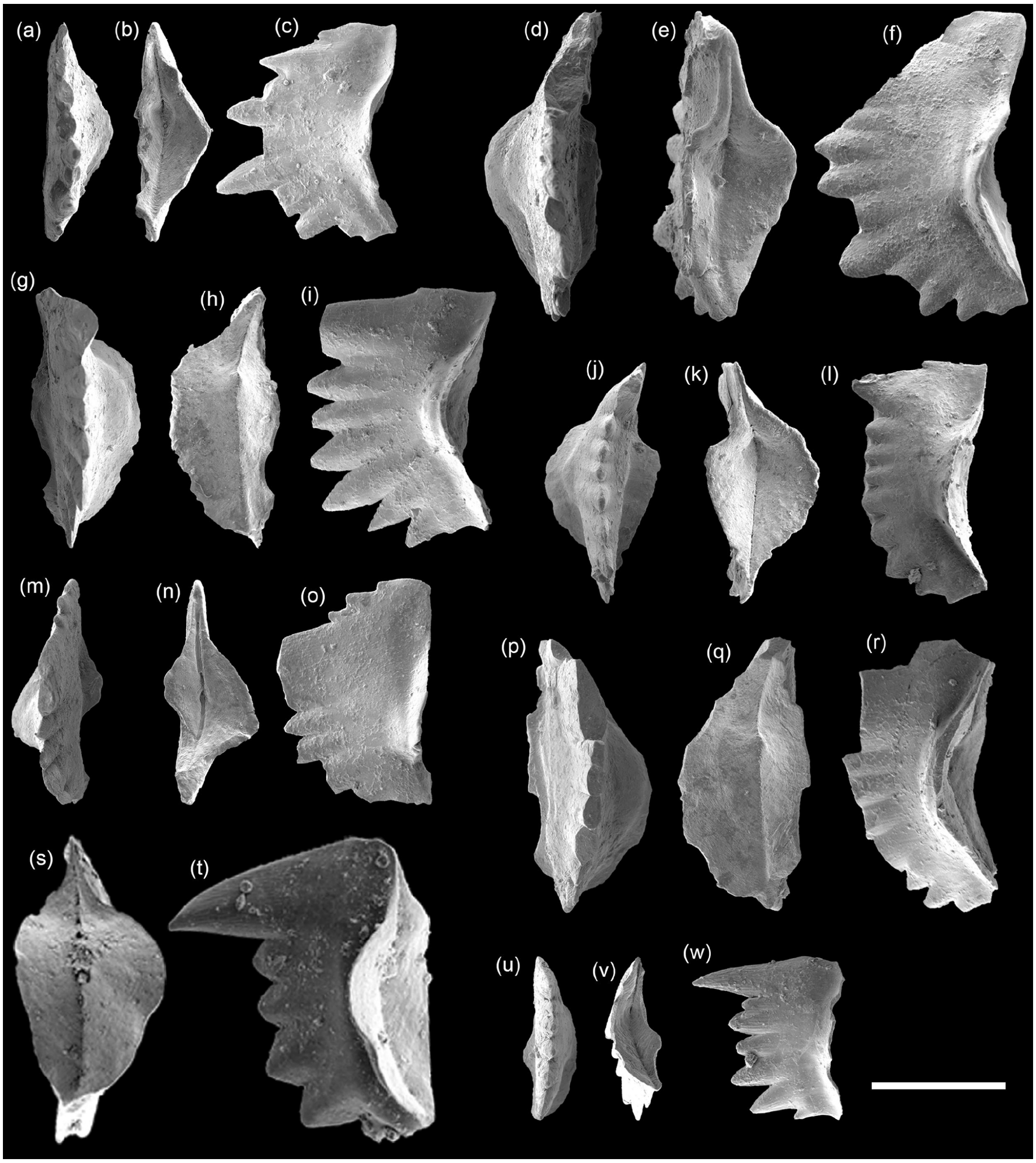

Figure 9. SEM photos of conodonts from the Changhsing and Daye formations, Zhangkouzi section. **(a–c)** *Hindeodus sosioensis* Kozur, 1996 P_1 element: 1050. Panels **(d)**–**(f)** and **(p)**–**(r)** are *Hindeodus* sp. P_1 elements: **(d–f)** 1051 and **(p–r)** 1052. Panels **(g)**–**(i)** and **(s)**–**(t)** are *Hindeodus parvus* Kozur, 1976 P_1 elements: **(g–i)** 1053 and **(s–t)** 1054. Panels **(j)**–**(o)** and **(u)**–**(w)** are *Hindeodus postparvus* Kozur, 1989 P_1 elements: **(j–l)** 1055, **(m–o)** 1056, and **(u–w)** 1057. Panels **(a)**–**(c)**, **(d)**–**(f)**, **(p)**–**(r)**, **(g)**–**(i)**, **(j)**–**(n)**, and **(u)**–**(w)** are from sample ZKZ-8, and panels **(s)**–**(t)** are from sample ZKZ2-8. The scale bar represents 200 µm.

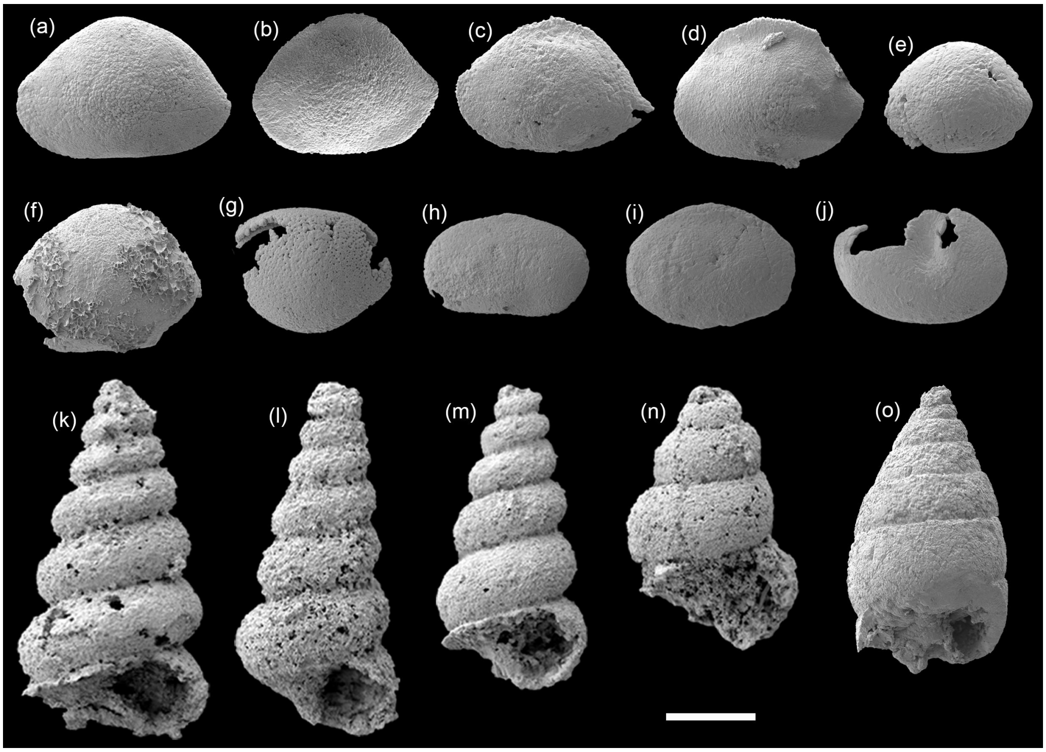

Figure 10. SEM photos of gastropods and ostracods from the Changhsing Formation, Zhangkouzi section. **(a–g)** *Bairdia* sp.: **(a)** 1058, **(b)** 1059, **(c)** 1060, **(d)** 1061, **(e)** 1062, **(f)** 1063, and **(g)** 1064. **(h–j)** *Darwinula* sp.: **(h)** 1065, **(i)** 1066, and **(j)** 1067. **(k–m)** *Polygyrina depressa* Wang and Xi, 1980: **(k)** 1068, **(l)** 1069, and **(m)** 1070. **(n–o)** *Polygyrina sichuanensis* Pan, 1982: **(n)** 1071 and **(o)** 1072. Panels **(a)**–**(f)** and **(o)** are from sample ZKZ2-1, panels **(g)**–**(j)** are from sample ZKZ2-2, and panels **(k)**–**(n)** are from sample ZKZ2-4. The scale bar represents 500 µm.

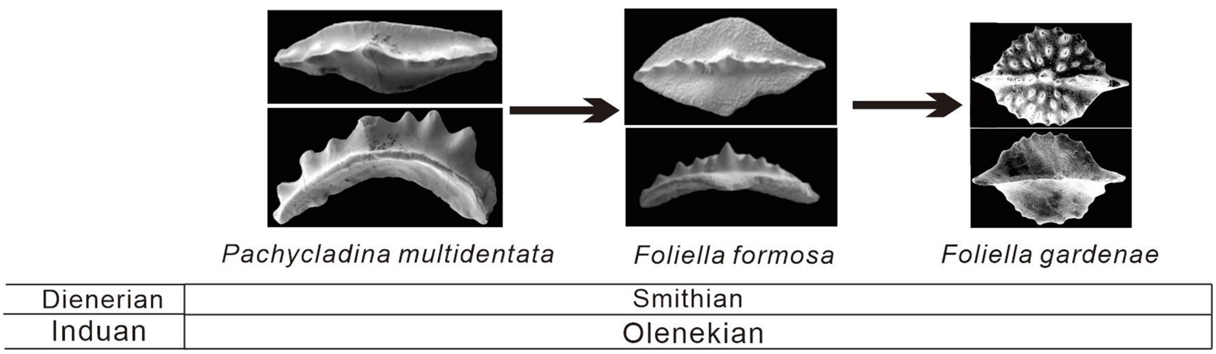

Figure 11. Evolutionary lineage of *Pachycladina* and *Foliella*. *Pachycladina multidentata* and *Foliella formosa* are documented from the Chencun section of Liangshan area. *Foliella gardenae* is taken from Kolar-Jurkovšek and Jurkovšek (1995).

Appendix A: Systematic palaeontology

Systematic descriptions of conodonts herein follow the classification established by Müller (1962), Budurov and Pantić (1973), Tian et al. (1983), Shigeta et al. (2009), Yuan and Shen (2011), Brosse et al. (2017), and Metcalfe and Crowley (2020). The apparatus notation (P_{1-2}, M, S_{0-4}) of Koike (2016) and Sun et al. (2020) is applied to elements of the family Ellisonidae.

Phylum Chordata Bateson, 1886

Subphylum Vertebratea Cuvier, 1812

Class Conodonta Pander, 1856

Order Prioniodinida Sweet, 1988

Family Ellisoniidae Clark, 1972

Genus *Foliella* Budurov and Pantić, 1973

Type species. *Polygnathus gardenae* Staesche, 1964.

Foliella formosa (Tian, 1983)
(Fig. 3a–r)

Diagnosis. The specimens are approximately 1–3 mm in size, resembling an oval leaf with a slightly narrower anterior end compared to the posterior end, and the entire unit is slightly arched in lateral view. In oral view, the cusp is in the middle part of the unit and is almost twice the size of other denticles. About 4 to 5 equally sized denticles are developed on each side of the cusp. There is an evenly distributed and separate nodular pattern on the platform. The aboral surface is concave and has pleural and obvious concentric growth lines.

Material. Six specimens

Age. Smithian

Occurrence. Daye Formation, Liangshan, Hanzhong, Shaanxi Province, South China

Remarks. Oral surface specimens, obtained from the Liangshan area, are relatively smooth, and the separate nodular pattern on the platform is obvious, consistent with the specimens of Tian (1983). Tian (1983) described the species as possessing a cusp in a subcentral position, flat denticles that are laterally fused, and an evenly distributed and separate nodular pattern on the oral surface. On the aboral surface there is no obvious basal pit (e.g. Tian 1983, pl. 82, figs. 3–6).

Budurov and Pantić (1973) described the morphological features of the genus *Foliella*: the overall shape of unit is like an oval leaf, with nodules distributed on platform and a keel through from the front to the back of the unit. The platform is basically symmetrical, with linear denticles distributed on the carina, and the cusp is located near the middle part of the unit that is slightly larger than other denticles.

Tian (1983) assigned this species to the genus *Gladigondolella*; however, we suggest that this species instead be assigned to the genus *Foliella*. Tian (1983) described the species "*formosa*" as possessing a cusp in a subcentral position, with low denticles that are laterally fused and an evenly distributed and separate nodular pattern on the oral surface. On the aboral surface there is no obvious basal pit. Besides, the genus *Pachycladina* has tall and strong denticles (Perri, 1987; Wu et al., 2021), which are clearly distinguished from genus *Foliella*. Therefore, through the above description and comparison of the characteristics of the genera *Foliella*, *Pachycladina*, and *Gladigondolella*, "*Gladigondolella*" *formosa* (Tian, 1983) is here suggested as belonging to the genus *Foliella*.

Genus *Pachycladina* Staesche, 1964

Type species *Pachycladina obliqua* Staesche, 1964

Remarks. Genus *Pachycladina* was originally established as a mono-element apparatus by Staesche (1964). Sweet (1981) constructed the apparatus of this genus with Pa, Pb, M, Sa, Sb, and Sc elements. Later Perri and Andraghetti (1987), Zhang and Yang (1991), Kolar-Jurkovšek (1996), Song (2012), and Wu et al. (2021) also described *Pa. obliqua* as seximembrate apparatus.

Diagnosis. The 15-element apparatus of *Pachycladina* is composed of seven different element types (4S, 1M, 2P), whose morphological description are as follows.

- The P_1 (Pa) element (Figs. 5a–x; 6a–f) is planate and has one or more large denticles of the same size as cusp in the unit. In aboral view, there is a keel without obvious furrow and basal pit.

- The P_2 (Pb) element is asymmetrical and digyrate (Fig. 6s). The element bears four to five laterally and posteriorly inclined discrete denticles.

- The M element (Fig. 6t, u) is digyrate, with two lateral processes of different lengths and a high cusp. There are five to six denticles on the posterior process.

- The S_0 (Sa) element is symmetrical and alate (Figs. 6g–l; 7a–k, t–v). There is an erect cusp on the middle of unit and two short processes with three to five denticles. The S_0 element of *Pachycladina* is biramous and different from other ellisonids (Koike, 2016), which are normally triramous. Our data confirm previous studies showing that the S_0 element of *Pachycladina* is biramous and not triramous (Sweet, 1981; Perri and Andraghetti, 1987).

- The $S_{1/2}$ (Sb) elements (Figs. 6m–r, v–x to 7o–s, w–y, z–ah) are asymmetrical and digyrate. There are four to five denticles on the anterior and two to three denticles on the posterior processes. The cusp and denticles tilt posteriorly.

- The $S_{3/4}$ (Sc) elements (Figs. 6y–ad, 7l–n) are asymmetrical. S_3 and S_4 are almost identical. Each element has two processes of different lengths, with three to four denticles on the anterior process and two to three denticles on the posterior process. The cusp is long and very stout, which is 2 or 3 times higher than other denticles.

Pachycladina costatus (Tian, 1983)
(Fig. 5a–f)

1983 *Latignathus costatus* Tian, p. 363–364, pl. 93, fig. 7.

Diagnosis. The P_1 element is slightly arched and has five to six separate wide denticles. In aboral view, there are concentric growth lines and a keel without a furrow and a basal pit.

Material. Three P_1 elements

Age. Smithian

Occurrence. Daye Formation, Liangshan, Hanzhong, Shaanxi Province, South China

Pachycladina magnus (Tian, 1983)
(Fig. 5g–l)

1983 *Latignathus magnus* Tian, p. 364, pl. 87, figs. 2, 5.

Diagnosis. The P_1 element is slightly arched and has five to seven separate, strong denticles on the well-developed platform. The first two denticles in the frontier part of the unit are relatively large, and there is a wide gap between these two bigger denticles. Other denticles are relatively small and evenly distributed behind those two large denticles.

Material. Two P_1 elements

Age. Smithian

Occurrence. Daye Formation, Liangshan, Hanzhong, Shaanxi Province, South China

Pachycladina bidentata Wang and Cao, 1981
(Fig. 5m–x)

1981 *Pachycladina bidentata* Wang and Cao, p. 368, pl. 3, figs. 3–5.

1993 *Pachycladina bidentata* Wang and Cao; Wang, p. 262, pl. 58, figs. 8, 10.

Diagnosis. The P_1 element has concentric growth lines in both lower and lateral views. In aboral view, there is a keel without a furrow and basal pit. The anterior process has a denticle that is equal in size to the cusp, and the posterior process has several smaller and shorter denticles compared with the cusp.

Material. Seven P_1 elements

Age. Smithian

Occurrence. Daye Formation, Liangshan, Hanzhong, Shaanxi Province, South China

Pachycladina multidentata Wang and Cao, 1981
(fig. 6a–f)

1981 *Pachycladina multidentata* Wang and Cao, p. 369, pl. 3, figs. 1–2.

1983 *Latignathus multidentatus* Tian, p. 364–365, pl. 87, fig. 3; pl. 89, fig. 2.

1993 *Pachycladina multidentata* Wang and Cao; Wang, p. 263, pl. 59, fig. 11.

Diagnosis. The P_1 (Pa) element (Fig. 6a–f) is planate, and the cusp is in the middle part of the unit. The anterior process is straight or curved, with at least three denticles that are almost the same size as the cusp. In aboral view, there is a keel without an obvious furrow and basal pit.

Material. 23 P_1 elements

Age. Smithian

Occurrence. Daye Formation, Liangshan, Hanzhong, Shaanxi Province, South China.

Data availability. The material can be accessed at the Department of Geology, Northwest University, Xi'an, China.

Author contributions. YZ collected and analysed the data and wrote the manuscript. YC provided supervisory support, analysed the data, and revised the manuscript. JW analysed the data and revised the manuscript. XM provided data and revised the manuscript. CX analysed the data and revised the manuscript. ZZ analysed the data and revised the manuscript. TT assisted with writing and structure and revised the manuscript. All the authors above have approved the manuscript and agreed to its submission. The content of this paper has not been published or accepted elsewhere and this manuscript has not been submitted to any other journal.

Competing interests. The contact author has declared that none of the authors has any competing interests.

Acknowledgements. We thank Viktor Karádi and Marc Leu for their review and constructive comments and suggestions, and we also thank Emanuela Mattioli for her help with editing this paper.

Financial support. This research was funded by the NSFC (grant nos. 42172013, 41720104002, 41890844, 41890843, 41930319, 42072003 and 41572002), the National Key Research and Development Program of China (grant no. 2023YFF0803601), and the 111 Project (grant no. D17013).

Review statement. This paper was edited by Emanuela Mattioli and reviewed by Marc Leu and Viktor Karádi.

References

Bateson, W.: Memoirs: the ancestry of the Chordata, J. Cell. Sci., 26, 535–572, https://doi.org/10.1242/jcs.s2-26.104.535, 1886.

Brosse, M., Baud, A., Bhat, G. M., Bucher, H., Leu, M., Vennemann, T., and Goudemand, N.: Conodont-based Griesbachian biochronology of the Guryul Ravine section (basal Triassic, Kashmir, India), Geobios, 50, 359–387, https://doi.org/10.1016/j.geobios.2017.10.001, 2017.

Budurov, K., and Pantié, S.: Die Conodonten der Campiller Schichten von Brassina (westserbien), II. Ststematischer Teil, Bulg. Acad. Sci. Geol. Inst. Ser. Paleontol., 22, 49–64 pls., 1–4, 1973.

Burgess, S. D., Bowring, S., and Shen, S. Z.: High-precision timeline for Earth's most severe extinction, P. Natl. Acad. Sci. USA, 111, 3316–3321, https://doi.org/10.1073/pnas.1317692111, 2014.

Chen, C. Z.: The base of Lower Triassic in southwest China, Ac. Stratigr. Sin., 2, 160–162, 1978.

Chen, C. Z., Li, W. B. and Ma, Q. H.: Triassic strata of southwest China, Science Press, Beijing, 5, 289–336, 1979.

Clark, D. L.: Early Permian crisis and its bearing on Permo-Triassic conodont taxonomy, Geol. Paleontol., 1, 147–158, 1972.

Cuvier, G.: Recherches sur les ossemens fossiles de quadrupèdes: où l'on rétablit les caractères de plusieurs espèces d'animaux que les révolutions du globe paroissent avoir détruites, 1, Deterville, 1812.

Dal Corso, J., Song, H., Callegaro, S., Chu, D. L., Sun, Y. D., Hilton, J., Grasby, S. E., Joachimski, M. M., and Wignall, P. B.: Environmental crises at the Permian–Triassic mass extinction, Nat. Rev. Earth Environ., 3, 197–214, https://doi.org/10.1038/s43017-021-00259-4, 2022.

Fan, J. X., Shen, S. Z., Erwin, D. H., Sadler, P. M., Macleod, N., Cheng, Q. M., Hou, X. D., Yang, J., Wang, X. D., Wang, Y., Zhang, H., Chen, X., Li, G. X., Zhang, Y. C., Shi, Y. K., Yuan, D. X., Chen, Q., Zhang, L. N., Li, C., and Zhao, Y. Y.: A high-resolution summary of Cambrian to Early Triassic marine invertebrate biodiversity, Science, 367, 272–277, https://doi.org/10.1126/science.aax4953, 2020.

Feng, X. Q., Chen, Z. Q., Woods, A., and Fang, Y. H.: A Smithian (Early Triassic) ichnoassemblage from Lichuan, Hubei Province, South China: Implications for biotic recovery after the latest Permian mass extinction, Palaeogeogr. Palaeocl., 486, 123–141, https://doi.org/10.1016/j.palaeo.2017.03.003, 2017.

Guo, J. F., Li, Y., Xiao, L., Li, X. C., Yao, X. Y, Zheng, Y. J., and Zhou, X. R.: Brachiopods from the wangpo shale (basal Lopingian, Permian) of Liangshan, southern Shaanxi Province, central China, Acta Palaeontol. Sin., 55, 192–206, 2016.

He, D. F., Guan, S. W., Zhang, S. C., and Sun, Y. P.: Formation and evolution of Later Paleozoic-Middle Triassic passive continental margin basin in the north part of Upper Yangtze Craton, Chin. J. Geol., 51, 329–353, https://doi.org/10.12017/dzkx.2016.002, 2016.

He, Y. B. and Luo, J. X.: Lithofacies palaeogeography of the Late Permian Changhsing Age in Middle and Upper Yangtze Region, J. Palaeogeogr., 12, 497–514, https://doi.org/10.7605/gdlxb.2010.05.001, 2010 (in Chinese).

Huang, B. C., Yan, Y. G., Piper, J. D. A., Zhang, D. H., Yi, Z. Y., Yu, S., and Zhou, T. H.: Paleomagnetic constraints on the paleogeography of the East Asian blocks during Late Paleozoic and Early Mesozoic times, Earth-Sci. Rev., 186, 8–36, https://doi.org/10.1016/j.earscirev.2018.02.004, 2018.

Huo, S. C.: The stratigraphy of the Liangshan area, south Shensi, with discussions of its geological history, Acta Geol. Sin., 1, 1960.

Jablonski, D.: Extinctions in the fossil record, Philos. T. R. Soc. Lond. B, 344, 11–17, https://doi.org/10.1098/rstb.1994.0045, 1994.

Jeppsson, L. and Anehus, R.: A new technique to separate conodont elements from heavier minerals, Alcheringa: An Australasian Journal of Palaeontology, 23, 57–62, https://doi.org/10.1080/03115519908619339, 1999.

Jeppsson, L., Fredholm, D., and Mattiasson, B.: Acetic acid and phosphatic fossils-a warning, J. Paleontol., 59, 952–956, 1985.

Jian, W. C., Teng, Z. H., Yin, F. J., Liu, H. F., Li, W. H., Zhou, D. W., Zhang, Y. X., Liu, Y. Q., Cui, Z. L., and Fu, J. H.: Liangshan geology, Northwest University Press, Xi' an, 184 pp., ISBN 50132001, 1992.

Jiang, H. S., Lai, X. L., Sun, Y. D., Wignall, P. B., Liu, J. B., and Yan, C. B.: Permian-Triassic conodonts from Dajiang (Guizhou, South China) and their implication for the age of microbialite deposition in the aftermath of the end-Permian mass extinction, J. Earth Sci. 25, 413–430, https://doi.org/10.1007/s12583-014-0444-4, 2014

Kanmera, K. and Nakazawa, K.: Permian-Triassic relationship and faunal changes in the eastern Tethys, Canad. Soc. Petrol. Geol, 2, 100–119, 1973.

Koike, T.: Multielement conodont apparatuses of the ellisonidae from Japan, Paleontol. Res., 20, 161–175, https://doi.org/10.2517/2016PR007, 2016.

Kolar-Jurkovšek, T.: Contribution to the knowledge of the Lower Triassic conodont fauna in Slovenia, Razprave IV, Razreda Sazu, 37, 3–21, 1996.

Kolar-Jurkovšek, T. and Jurkovšek, B.: Lower Triassic conodont fauna from Trzic (Karavanke Mts. Slovenia), Eclogae Geol. Helv., 88, 789–801, https://doi.org/10.5169/seals-167704, 1995.

Kolar-Jurkovšek, T. and Jurkovšek, B.: Konodonti Slovenije/Conodonts of Slovenia, Geološki zavod Slovenije, Ljubljana, 169 pp., ISBN 9789616498661, 2019.

Kozur, H. W.: The taxonomy of the gondolellid conodonts in the Permian and Triassic, Cour. For. Senckenb., 117, 409–469, 1989.

Kozur, H. W.: The conodonts *Hindeodus*, *Isarcicella* and *Sweetohindeodus* in the uppermost Permian and lowermost Triassic, Geol. Croat., 49, 81–115, https://doi.org/10.4154/GC.1994.45, 1996.

Kozur, H. W.: Integrated ammonoid, conodont and radiolarian zonation of the Triassic and some remarks to Stage/Substage subdivision and the numeric age of the Triassic stages, Albertiana, 28, 57–74, 2003.

Kozur, H. W. and Pjatakova, M.: Die Conodontenart *Anchignathodus parvus* n. sp. eine wichtige Leitform der basalen Trias, Koninklijke Nederlandse Akademie van Wetenschappen, Amsterdam, Proc. Ser. B, 79, 123–128, 1976.

Liu, B. P., Quan, Q. Q., Feng, Q. L., Zhao, X. W., and Zhou, Z. G.: A course in geohistory, Geology Press, Beijing, 277 pp., ISBN 9787116021129, 1996.

Liu, H. F.: Upper Permian Changxing Formation in Liangshan region of Nanzheng, Shaanxi, Journal of Northwest University (Natural Science Edition), 4, 63–70, 1982.

Lu, Y. H.: On the stratification and correlation of the Permian in southern China and in the Liangshan area of Hanzhong, Acta Geol. Sin., 36, 159–193, http://ir.nigpas.ac.cn/handle332004/7353 (last access: 19 September 2024) 1956.

Lyu, Z. Y., Henderson, C. M., Chen, Z. Q., Tong, J. N., Zhao, L. S., Han, C., and Wu, S. L.: High-resolution conodont unitary association zonations (UAZs) across the Induan-Olenekian boundary (Lower Triassic): A global correlation, Palaeogeogr. Palaeocl., 627, 111721, https://doi.org/10.1016/j.palaeo.2023.111721, 2023.

Maekawa, T., Komatsu, T., Shigeta, Y., Dang, T. H., and Nguyen, D. P.: Upper Induan and lower Olenekian conodont assemblages from the lowest part of the Bac Thuy Formation in the Ban Ru area, northeastern Vietnam, 193–207, 2016

Metcalfe, I. and Crowley, J. L.: Upper Permian and Lower Triassic conodonts, high-precision U-Pb zircon ages and the Permian-Triassic boundary in the Malay Peninsula, J. Asian Earth Sci., 199, 104403, https://doi.org/10.1016/j.jseaes.2020.104403, 2020.

Miao,Y., Tian,Y. F., Wu, L., Lu, X. C., Li, S. Z., and Song, W. T.: Zircon U-Pb chronology, petrochemistry and its implications for Rodinia supercontinent tectonic evolution in the Lower Triassic Feixianguan Formation in the Daibu area, southwest of upper Yangtze, Acta Geol. Sin., 3739–3757, https://doi.org/10.19762/j.cnki.dizhixuebao.2021067, 2021.

Müller, K. J.: Zur systematischen Einteilung der Conodontophorida, Paläont. Z., 36, 109–117, https://doi.org/10.1007/BF02989634, 1962.

Orchard, M. J.: Conodont diversity and evolution through the latest Permian and Early Triassic upheavals, Palaeogeogr. Palaeocl., 252, 93–117, https://doi.org/10.1016/j.palaeo.2006.11.037, 2007.

Pan, H. Z.: Triassic marine fossil gastropods from southwest China, Bulletin of the Nanjing Institute of Geology and Palaeontology, Academia Sinica, 4, 153–188, 1982.

Pander, C. H.: Monographie der fossilen fische des silurischen systems der Russisch-baltischen gouvernements, St. Petersburg (Akademie der Wissenschaften), 91 pp., ISBN 9780341383277, 1856.

Perri, M. C.: Conodont biostratigraphy of the Werfen Formation (Lower Triassic), southern Alps, Italy, Bolletino della Societa Paleontologica Italiana, 30, 23–46, 1991.

Perri, M. C. and Andraghetti, M.: Permian–Triassic boundary and Early Triassic conodonts from the Southern Alps, Italy, Riv. Ital. Paleontol. Stratigr., 93, 291–328, https://doi.org/10.54103/2039-4942/13193, 1987.

Raup, D. M.: Size of the Permo-Triassic bottleneck and its evolutionary implications, Science, 206, 217–218, https://doi.org/10.1126/science.206.4415.217, 1979.

Retallack, G. J.: Permian–Triassic life crisis on land, Science, 267, 77–80, https://doi.org/10.1126/science.267.5194.77, 1995.

Rui, L., Zhao, J. M., Mu, X. N., Wang, K. L., and Wang, Z. H.: Restudy of Wuchiaping Limestone in Liangshan, Hanzhong, Shaanxi Province, J. Stratigr., 8, 179–193, https://doi.org/10.19839/j.cnki.dcxzz.1984.03.002, 1984.

Shen, B. H., Shen, S. Z., Hou, Z. S., Wu, Q., Zhang, S. C., Zhang, B., Zhang, Y. C., and Yuan, D. X.: Lithostratigraphic subdivision and correlation of the Permian in China, J. Stratigr., 45, 319–339, https://doi.org/10.19839/j.cnki.dcxzz.2021.0027, 2021.

Shen, S. Z., Crowley, J. L., Wang, Y., Bowring, S. A., Erwin, D. H., Sadler, P. M., Cao, C. Q., Rothman, D. H., Henderson, C. M., Ramezani, J., Zhang, H., Shen, Y., Wang, X. D., Wang, W., Mu, L., Li, W. Z., Tang, Y. G., Liu, X. L., Liu, L. J., Zeng, Y., Jiang, Y. F., and Jin, Y. G.: Calibrating the end-Permian mass extinction, Science, 334, 1367–1372, https://doi.org/10.1126/science.1213454, 2011.

Shen, S. Z., Ramezani, J., Chen, J., Cao, C. Q., Erwin, D. H., Zhang, H., Xiang, L., Schoepfer, S. D., Henderson, C. M., Zheng, Q. F., Bowring, S. A., Wang, Y., Li, X. H., Wang, X. D., Yuan, D. X., Zhang, Y. C., Mu, L., Wang, J., and Wu, Y. S.: A sudden end-Permian mass extinction in South China, Geol. Soc. Am. Bull., 131, 205–223, https://doi.org/10.1130/B31909.1, 2019.

Shigeta, Y., Zakharov, Y. D., Maeda, H., and Popov, A. M.: The Lower Triassic System in the Abrek Bay area, south Primorye, Russia, National Museum of Nature and Science, 218 pp., ISSN: 1342-9574, 2009.

Song, H. J. and Tong, J. N.: Mass extinction and survival during the Permian-Triassic crisis, Earth Sci., 41, 901–918, https://doi.org/10.3799/dqkx 2016.077, 2016.

Song, H. J., Wignall, P. B., and Dunhill, A. M.: Decoupled taxonomic and ecological recoveries from the Permo-Triassic extinction, Sci. Adv., 4, eaat5091, https://doi.org/10.1126/sciadv.aat5091, 2018.

Song, H. J., Wignall, P. B., Chu, D. L., Tong, J. N., Sun, Y. D., Song, H. Y., He, W. H., and Tian, L.: Anoxia/high temperature double whammy during the Permian-Triassic marine crisis and its aftermath, Sci. Rep.-UK, 4, 4132, https://doi.org/10.1038/srep04132, 2014.

Song, H. J, Wignall, P. B., Tong, J. N., and Yin, H. F.: Two pulses of extinction during the Permian-Triassic crisis, Nat. Geosci., 6, 52–56, https://doi.org/10.1038/NGEO1649, 2013.

Song, X. T.: The Lower Triassic conodonts and its biostratigraphy at the Guan Ziba section, Wangcang, Sichuan Basin, M. S. thesis, China University of Geosciences, Beijing, 52 pp., 2012.

Staesche, U.: Conodonten aus dem Skyth von Südtirol, Neues Jahrbuch für Geologie und Paläontologie, Abhandlungen, 119, 247–306, 1964.

Stanley, S. M.: Estimates of the magnitudes of major marine mass extinctions in earth history, P. Natl. A. Sci. USA, 113, E6325–E6334, https://doi.org/10.1073/pnas.1613094113, 2016.

Sun, Z. Y., Liu, S., Ji, C., Jiang, D. Y., and Zhou, M.: Synchrotron-aided reconstruction of the prioniodinin multi-element conodont apparatus (*Hadrodontina*) from the Lower Triassic of China, Palaeogeogr., Palaeocl., 560, 109913, https://doi.org/10.1016/j.palaeo.2020.109913, 2020.

Sweet, W. C.: Family Ellisonidae Clark, 1972, in: Treatise on Invertebrate Paleontology, edited by: Robinson, R. A., Pt. W, Miscellanea, Supplement 2, Conodonta, W152–W154, Geological Society of America, Boulder and University of Kansas Press, Lawrence, ISBN: 0-8137-3028-7, 1981.

Sweet, W. C.: The Conodonta, Morphology, taxonomy, paleoecology, and evolutionary history of a long-extinct animal phylum, Oxford Monographs on Geology and Geophysics 10, 224 pp., New York (Oxford University Press), ISBN 0-19-504352-9, 1988.

Tian, C. R., Dai, J., and Tian, S. G.: Triassic conodonts, in: Chengdu Institute of Geology and Mineral Resources, Paleontological atlas of southwest China, Volume of microfossils, Geol. Publ. House, Beijing, 802 pp., ISBN: 15038 886, 1983.

Tong, J. N., Zakharov, Y. D., Orchard, M. J., Yin, H. F., and Hansen, H. J.: A candidate of the Induan-Olenekian boundary stratotype in the Tethyan region, Sci. China Ser. D, 46, 1182–1200, https://doi.org/10.3969/j.issn.1674-7313.2003.11.010, 2003.

Wang, C. Y.: Conodonts of lower Yangtze valley – an indexes to biostratigraphy and organic metamorphic maturity, Science Press, Beijing, 386 pp., ISBN 7030034627, 1993.

Wang, H. J., and Xi, Y.: Late Permian – Early Triassic gastropods of western Guizhou, Stratigraphy and Palaeontology of Upper Permian coal bearing formation in western Guizhou and eastern Yunnan, China, Science Press, Beijing, 195–240, ISBN 130311197, 1980.

Wang, Z. H.: Permian-Lower Triassic conodonts of the Liangshan area, southern Shaanxi, Ac. Palaeontol. Sin., 17, 115–155, 1978.

Wang, Z. H. and Cao, Y. Y.: Early Triassic conodonts from Lichuan, western Hubei, Acta Palaeontol. Sin., 20, 363–375, https://doi.org/10.19800/j.cnki.aps.1981.04.010, 1981.

Wu, G. C., Ji, Z. S., Liao, W. H., and Yao, J. X.: New biostratigraphic evidence of Late Permian to Late Triassic deposits from central Tibet and their paleogeographic implications, Lithosphere, 11, 683–696, https://doi.org/10.1130/L1046.1, 2019.

Wu, G. C., Ji, Z. S., Kolar-Jurkovšek, T., Yao, J. X., and Lash, G. G.: Early Triassic *Pachycladina* fauna newly found in the southern Lhasa Terrane of Tibet and its palaeogeographic implications, Palaeogeogr. Palaeocl., 562, 110030, https://doi.org/10.1016/j.palaeo.2020.110030, 2021.

Wu, W. S.: Upper Permian corals from Liangshan, S. Shensi. Acta Palaeontol. Sin., 5, 325–342, 1957.

Xu, D., Dieter, K., and Song, H. J.: Morphological selectivity of the Permian-Triassic ammonoid mass extinction, Geology, 49, 1112–1116, https://doi.org/10.1130/G48788.1, 2021.

Yang, B., Lai, X. L., Wignall, P. B., Jiang, H. S., Yan, C. B., and Sun, Y. D.: A newly discovered earliest Triassic chert at Gaimao section, Guizhou, southwestern China, Palaeogeogr. Palaeocl., 344, 69–77, https://doi.org/10.1016/j.palaeo.2012.05.019, 2012.

Yin, H. F., Zhang, K. X., Tong, J. N., Yang, Z. Y., and Wu, S. B.: The Global Stratotype Section and Point (GSSP) of the Permian–Triassic Boundary, Episodes, 24, 102–114, https://doi.org/10.18814/epiiugs/2001/v24i2/004, 2001

Yuan, D. X. and Shen, S. Z.: Conodont succession across the Permian-Triassic boundary of the Liangfengya section, Chongqing, South China, Acta Palaeontol. Sin., 50, 420–438, https://doi.org/10.19800/j.cnki.aps.2011.04.002, 2011.

Zhang, G. W., Zhang, B. R., Yuan, X. C., and Xiao, Q. H.: Qinling orogenic belt and continental dynamics, Science Press, Beijing, 855 pp., ISBN 7030088689, 2001.

Zhang, G. W., Dong, Y. P., Lai, S. C., Guo, A. L., Meng, Q. R., Liu, S. F., Cheng, S. Y., Yao, A. P., Zhang, Z. Q., and Pei, X. Z.: Mianlüe tectonic zone and Mianlüe suture zone on southern margin of Qinling-Dabie orogenic belt, Sci. China Ser. D, 47, 300–316, https://doi.org/10.1360/02yd0526, 2004.

Zhang, J. and Tong, J., N.:Vermicular limestone of the Lower Triassic and its origin in lower Yangtze Region, J. Palaeogeogr., 12(5), 14, https://doi.org/10.7605/gdlxb.2010.05.004, 2010.

Zhang, S. X. and Yang, Z. Y.: On multielement taxonomy of the Early Triassic conodonts, Stratigraphy and Paleontology of China, 1, 17-47, 1991.

Zhao, L. S., Orchard, M. J., Tong, J. N., Sun, Z. M., Zuo, J. X., Zhang, S. X., and Yun, A. L.: Lower Triassic conodont sequence in Chaohu, Anhui Province, China and its global correlation, Palaeogeogr. Palaeocl., 252, 24–38, https://doi.org/10.1016/j.palaeo.2006.11.032, 2007.

Zhao, L. S., Tong, J. N., Sun, Z. M., and Orchard, M. J.: A detailed Lower Triassic conodont biostratigraphy and its implications for the GSSP candidate of the Induan–Olenekian boundary in Chaohu, Anhui Province, Prog. Nat. Sci., 18, 79–90, https://doi.org/10.1016/j.pnsc.2007.07.001, 2008.

Zhao, X. M, Tong, J. N., Yao, H. Z., Niu, Z. J., Luo, M., Huang, Y. F., and Song, H. J.: Early Triassic trace fossils from the Three Gorges area of South China: Implications for the recovery of benthic ecosystems following the Permian-Triassic extinction, Palaeogeogr. Palaeocl., 429, 100–116, https://doi.org/10.1016/j.palaeo.2015.04.008, 2015.

Zheng, B. S., Mou, C. L., Wang, X. P., and Chen, H. D.: U-Pb ages, trace elements and Hf isotopes of detrital zircons from the Late Permian-Early Triassic sedimentary succession in the northern Yangtze Block, South China: Implications for the reconstruction of the South China Block in Pangea, J. Asian Earth Sci., 206, 104609, https://doi.org/10.1016/j.jseaes.2020.104609, 2021.